INTERNATIONAL JOURNAL OF CLIMATOLOGY
Int. J. Climatol. **24**: 341–360 (2004)
Published online 11 February 2004 in Wiley InterScience (www.interscience.wiley.com). DOI: 10.1002/joc.1005

A STUDY ON DYNAMIC AND THERMODYNAMIC ASPECTS OF BREAKS IN THE SUMMER MONSOON OVER INDIA

R. BHATLA, U. C. MOHANTY,* P. V. S. RAJU and O. P. MADAN
Centre for Atmospheric Sciences, Indian Institute of Technology, Hauz Khas, New Delhi 110 016, India

Received 2 June 2003
Revised 28 November 2003
Accepted 28 November 2003

ABSTRACT

The rainfall associated with the Indian summer monsoon shows large intraseasonal and interannual variability. Break-monsoon conditions are one of the important epochs of the monsoon, and they contribute significantly to the intraseasonal variability of the monsoon. The National Centers for Environmental Prediction–National Center for Atmospheric Research reanalysis data sets are used to investigate the significant energy budget terms during the pre-break (5 days prior to the commencement of the break), break and post-break (5 days after the cessation of the break) periods. In the present study, certain dynamic and thermodynamic characteristics of the monsoon circulation during break-monsoon conditions are investigated. The important terms in the various energy budget equations are analysed between the surface and 100 hPa for the break and its departures from pre- and post-break for the period 1968–96. The statistical significance of these departures is also examined by Student's t-test at the 95% confidence level. The volume integral of the budget terms is also examined in four sectors, i.e. the Arabian Sea, Bay of Bengal, northern India and central India.

Significant changes in the wind field and vorticity at 850 hPa take place in the monsoon trough zone, coastal regions of the western coast of India and the southwestern Bay of Bengal off the southern Indian coast. The vertically upward rising arm of the Hadley cell weakens during the break phase. The strong flux convergence of kinetic energy in the central Arabian Sea and flux divergence in the northeastern Bay of Bengal weakens during pre- and post-break periods. Significant changes in the diabatic heating horizontal flux of heat and moisture are observed in the monsoon trough zone, central and northwestern Bay of Bengal. The Bay of Bengal and central India sectors show higher magnitudes and changes in respect of dynamic and thermodynamic parameters compared with the Arabian Sea and northern India.

KEY WORDS: summer monsoon; break-monsoon; reanalysis; energetics; Student's t-test

1. INTRODUCTION

The Indian summer monsoon has brought welcome rain to India with almost unremitting regularity for thousands of years. The onset of the Indian summer monsoon, its activity during the season and its withdrawal show large variations from year to year. The southwest summer monsoon over India undergoes periods of enhanced and reduced rainfall activity, and these intraseasonal variations are termed as 'active' and 'weak' monsoon phases respectively. Sometimes, during a 'weak' phase of the monsoon, the monsoon trough is found to shift northward from its normal position to the foothills of the Himalayas (Ramamurthy, 1969; Rao, 1976) and the precipitation activity over the country becomes considerably subdued, except over some parts of the country such as the foothills of the Himalayas, northeastern Indian states and Tamil Nadu where rainfall activity increases. Such a situation is known as a 'break' in the southwest summer monsoon over India. A prolonged break situation in the monsoon is associated with extreme heat stress for agricultural crops, reduced water supply to reservoirs and a reduction in the generation of hydroelectricity, which affects the country's economy.

* Correspondence to: U. C. Mohanty, Centre for Atmospheric Sciences, IIT-Delhi, Hauz Khas, New Delhi 110 016, India;
e-mail: mohanty@cas.iitd.ernet.in

Ramamurthy (1969) studied 80 years (1888–1967) of rainfall data and suggested that most of the breaks had durations of 3–5 days. Some very long-duration break periods lasted for 17–20 days, and the few such types of prolonged break occurred mainly during August. Ramaswamy (1962) noticed that break periods are influenced by the intrusion of the mid-latitude trough into the Indo-Pakistan region in the middle and upper troposphere. The atmospheric general circulation in both hemispheres was locked in a low-index Rossby regime during intensely weak phases of the Indian summer monsoon (Ramaswamy and Pareek 1978). Unninayar and Murakami (1978) showed that a bifurcation of the Tibetan high under the influence of a mid-latitude trough near the Indo-Pakistan region resulted in weak monsoon periods. Raman and Rao (1981) noted that changes associated with a weak monsoon included the occurrence of a stagnant blocking ridge in the upper troposphere from 90 to 115 °E over East Asia. Ramamurthy (1969) catalogued the breaks in July and August during 1888 to 1967 based on a persistent synoptic pattern (of at least 2 days length) in which the monsoon trough was absent in the sea-level chart, as well as up to 850 hPa. Krishnamurti and Ardanuy (1980) found that break-monsoon spells were associated with westward-propagating trough–ridge systems that had a periodicity of about 10–20 days using 40 years (1933–72) of surface pressure data.

Rodwell (1997) illustrated that breaks in the Indian summer monsoon could be triggered by extratropical weather systems in Southern Hemisphere. The effect of the large-scale heat and moisture budget on the onset and activities of the summer monsoon was investigated by Mohanty *et al.* (1982a,b). In a recent study, Krishnan *et al.* (2000) presented results on the diagnostic analysis of observation and complementary experiments with a simple numerical model that enabled them to synthesize the morphology and dynamics of breaks in the Indian summer monsoon. Through modelling experiments, it was demonstrated that low-latitude Rossby wave dynamics in the presence of a monsoon basic flow, which is driven by a steady north–south differential heating, is the primary physical mechanism that controls the so-called monsoon breaks (Krishnan *et al.*, 2000).

Earlier studies about the break condition have revealed the shifting of the monsoon trough line to the Himalayan foothills, the absence of easterlies over the northern parts of the country up to 1.5 km a.s.l., and the presence of a trough in mid- and upper-tropospheric westerlies over northern parts of the country as being some of the important features. In addition to this, the movement of the cyclonic circulation over low latitudes, e.g. over the southwest Bay of Bengal or over southern Tamil Nadu (Koteswaram, 1950; Mukherjee and Natarajan, 1968), the presence of a trough in mid- and upper-tropospheric westerlies over northern parts of the country (Pisharoty and Desai, 1956), a weak pressure gradient over the west coast, and sometimes isobars running parallel to the west coast (Malurkar, 1950), strong westerly winds in the northern parts of the country compared with the westerlies over the peninsula are some of the important features during most of the break situations. During the break-monsoon, considerable reductions in precipitation and cloudiness, coupled with wind changes, suggest the need for examination of the changes over the Indian seas, which are considered to be the source of moisture and hence diabatic energy for the maintenance of the monsoon system over the Indian subcontinent. Therefore, the aim of this paper is to examine the changes in circulation characteristics, dynamics and thermodynamics over India and the adjoining seas that lead to break-situation aspects in the summer monsoon. The availability of reliable and homogeneous global National Centers for Environmental Prediction–National Center for Atmospheric Research (NCEP–NCAR) reanalysis data facilitates the carrying out of a composite study of break cases (1968–96) in the context of changes in circulation, diagnostics and energetics associated with the pre-break situation to the break and from the break situation to the revival phase of the monsoon.

2. DATA AND METHODOLOGY

Information concerning the break-monsoon situation (Table I) was obtained from scientific reports of the India Meteorological Department (De *et al.*, 1998) for the period 1968–96. Short breaks, lasting for only 1 or 2 days, are not taken into account. In the present study, break-monsoon situations that lasted for 3 days or more are considered. Thus, a total of 33 breaks form the basis of the present study (Table I).

In order to study the dynamic and thermodynamic characteristics of break-monsoon conditions with changes in circulation and energetics, a reliable, consistent and quality-controlled data set is needed over the Indian

Table I. Pre-break, break and post-break periods from 1968 to 1996

Year	Pre-break period	Break period	Post-break period
1968	20–24 August	25–29 August	30 August–3 September
1969	12–16 August	17–20 August	21–25 August
	20–24 August	25–27 August	28 August–1 September
1970	7–11 July	12–25 July	26–30 July
1971	12–16 August	17–20 August	21–25 August
1972	12–16 July	17 July–3 August	4–8 August
	27–31 August	1–6 September	7–11 September
1973	18–22 July	23 July–1 August	2–6 August
1974	25–29 August	30 August–3 September	4–8 September
1975	19–23 July	24–28 July	29 July–2 August
1977	10–14 August	15–18 August	19–23 August
1978	11–15 July	16–21 July	22–26 July
1979	12–16 July	17–23 July	24–28 July
	10–14 August	15 August–3 September	4–8 September
1980	12–16 July	17–20 July	21–25 July
1981	21–25 July	26–30 July	31 July–4 August
	18–22 August	23–27 August	28 August–1 September
1983	17–21 August	22–25 August	26–30 August
1984	15–19 July	20–24 July	25–29 July
1985	17–21 August	22–25 August	26–30 August
1986	18–22 August	23–26 August	27–31 August
	24–28 August	29 August–3 September	4–8 September
1987	23–27 July	28 July–1 August	2–6 August
1988	30 June–4 July	5–8 July	9–13 July
	8–12 August	13–15 August	16–20 August
1989	5–9 July	10–12 July	13–17 July
	24–28 July	29–31 July	1–5 August
1990	3–7 July	8–10 July	11–15 July
	22–26 July	27–31 July	1–5 August
1991	29 August–2 September	3–9 September	10–14 September
1993	14–18 July	19–21 July	22–26 July
1995	7–11 August	12–15 August	16–20 August
1996	26 June–30 June	1–5 July	6–10 July

region. One such reliable and homogeneous global meteorological data set, which recently became available, is the NCEP–NCAR reanalysis (Kalnay *et al*., 1996). The data set is the result of a cooperative effort by NCEP and NCAR to produce 50 years (1948–97) of consistent and reliable global reanalysis of the atmospheric fields to support the needs of the research and climate monitoring community. The effort involves the recovery of land surface, ship, rawinsonde, aircraft, satellite and delayed mode Global Telecommunications System data, quality control and assimilation with a four-dimensional data assimilation system that is kept unchanged over the entire period (Kalnay *et al*., 1996). From this global data set, data for the duration of all break situations, as well as for 5 days prior to the commencement of a break in the monsoon (i.e. pre-break) and 5 days after the cessation of break/revival of normal monsoon (i.e. post-break) are extracted for the period 1968 to 1996. The region covered is 15 °S–45 °N, 30–120 °E. Based on 00 UTC and 12 UTC daily analysis, daily averages were computed in respect of zonal wind u, meridional wind v, geopotential height z, temperature T and specific humidity q at 12 mandatory pressure levels (1000, 925, 850, 700, 600, 500, 400, 300, 250, 200, 150 and 100 hPa). Further, the composite of basic fields and energetic terms of all 33 cases of break situations are computed for the pre-break, break and post-break periods. The vertical velocity fields in this study have been computed from horizontal wind components (u and v) by using the kinematics method suggested by O'Brien

(1970). In this technique, the divergence is adjusted to its vertically integrated value over the entire column of the atmosphere, i.e. to zero. To avoid problems with the divergent wind and estimation of budget terms with consistency, the vertical velocity field is estimated using the kinematics method, in which the divergence is adjusted in the vertical column of the atmosphere to be zero. Further, it is found that the vertical velocity obtained from the kinematics method delineates a more realistic Hadley circulation over the monsoon domain than do the archived fields. Hence, we resorted to that process. The following equations are used to calculate some of the energy budget terms.

The kinetic energy (KE) budget equation in the flux form may be written as

$$\frac{\partial K}{\partial t} + \nabla \cdot \mathbf{V}K + \frac{\partial(\boldsymbol{\omega}K)}{\partial p} = -\mathbf{V} \cdot \nabla\phi + \mathbf{V} \cdot \mathbf{F} \tag{1}$$

where K is the KE, $\mathbf{V}$ is a two-dimensional wind vector, $\boldsymbol{\omega}$ is vertical velocity, ϕ is geopotential and $\mathbf{F}$ is the frictional force. The first term on the left-hand side in Equation (1) denotes the local rate of change of the KE. The second term describes the horizontal flux divergence of the KE, and the third term indicates the vertical flux divergence of the KE. Similarly, the first term on the right-hand side of Equation (1) denotes the conversion of potential energy into KE through the action of pressure forces (adiabatic generation of KE). The last term signifies the dissipation of KE by turbulent frictional processes and is usually estimated as a residual. In fact, it is a sink or disappearance of KE from the observed scales of motion, which could be interpreted as the net loss of KE that has been input into the various scales of motion.

The vorticity budget equation is expressed as

$$\frac{\partial \zeta}{\partial t} + \nabla \cdot \mathbf{V}\zeta + \beta\mathbf{V} + \frac{\partial}{\partial p}(\zeta\boldsymbol{\omega}) = -(\zeta + f)D - k \cdot \left(\nabla\boldsymbol{\omega} \times \frac{\partial \mathbf{V}}{\partial p}\right) + z \tag{2}$$

where f is the Coriolis parameter, k is the unit vector, and

$$\beta = \frac{\partial f}{\partial y}$$

$$\zeta = \frac{\partial v}{\partial x} - \frac{\partial u}{\partial y}$$

is the relative vorticity and

$$D = \frac{\partial u}{\partial x} + \frac{\partial v}{\partial y}$$

is the divergence.

The first term on the left-hand side in Equation (2) is the time rate of change of vorticity. The second and third terms represent the horizontal fluxes of the relative and planetary vorticities. The fourth term describes the vertical flux of vorticity. Similarly, the first term on the right-hand side indicates the vorticity generation due to stretching. The second term indicates the vorticity generation due to tilting. The final term designates the residue of vorticity (i.e. generation or dissipation from sub-grid-scale processes).

The heat budget equation in the flux form can be written as

$$\frac{\partial(CpT)}{\partial t} + \nabla \cdot (\mathbf{V}CpT) + \frac{\partial}{\partial p}(\boldsymbol{\omega}CpT) - \boldsymbol{\omega}\alpha = Q_{\mathrm{H}} \tag{3}$$

where the first term on the left-hand side denotes the time rate of change of enthalpy. The second and third terms designate the horizontal and vertical fluxes of heat. The fourth term indicates adiabatic conversion of available potential energy (APE) to KE. The right-hand term describes the diabatic heating due to radiation, condensation and evaporation of falling raindrops and turbulent transfer of sensible heat and estimated as a residual.

The moisture budget equation in the flux form can be written as

$$\frac{\partial}{\partial t}(Lq) + \nabla \cdot (Lq\mathbf{V}) + \frac{\partial}{\partial p}(Lq\boldsymbol{\omega}) = Q_{\mathrm{L}} \tag{4}$$

The first term on the left-hand side of Equation (4) indicates the time rate of change of moisture. The second and third terms designate the horizontal and vertical moisture fluxes respectively. The right-hand term denotes the diabatic heating due to latent heat released or absorbed from evaporation and condensation, as well as turbulent transfer of latent heat.

All budget terms at each regular latitude/longitude grid point are computed and averaged, both in the zonal and meridional directions, over various sectors/zones and integrated vertically from the 1000 hPa to the 100 hPa tropospheric layers. Thus, the volume integral of any variable $F(\lambda, \varphi, P)$ for the limited region bounded by meridians λ_1 and λ_2, latitude circles φ_1 and φ_2 and isobaric surfaces P_1 and P_2 may be written as

$$\overline{F} = \frac{1}{g}\int_{\lambda_1}^{\lambda_2}\int_{\varphi_1}^{\varphi_2}\int_{P_1}^{P_2} Fa^2 \cos\varphi \mathrm{d}\lambda \mathrm{d}\varphi \mathrm{d}P$$

where a is the average radius of the Earth and g is the acceleration due to gravity.

The vertical integration of all the budget equations with the boundary condition that vertical motion ($\boldsymbol{\omega} = 0$) vanishes at the bottom and the top of the atmosphere leads to the elimination of all the terms representing vertical flux divergences of various quantities.

3. RESULTS AND DISCUSSIONS

In the present study, circulation features and all terms in various budget equations are evaluated between the surface and 100 hPa for the break period and its departure from pre-break (5 days before the break) and post-break (5 days after the break) periods. These departures have been tested for their significance using Student's t-test at the 95% level of confidence and are shaded in all results (Figures 2 to 11). Further, the volume integrals of the budget terms are examined in four significant sectors/regions, namely the Arabian Sea (AS; 50–72.5 °E, 5–15 °N), Bay of Bengal (BOB; 82.5–95 °E, 7.5–17.5 °N), northern India (NI; 75–90 °E, 22.5–30.0 °N) and central India (CI; 72.5–85 °E, 17.5–22.5 °N) as shown in Figure 1. The boxes were chosen to include areas where some of the controlling components of the monsoon (such as low-level jet (LLJ) in the Arabian Sea, the monsoon trough over the Indo Gangetic plain, monsoonal disturbances in the Bay of Bengal and their subsequent tracks of movement, etc.) are prominent and regions where significant changes occur from pre-break to break to post-break monsoon situations. Though we have examined all the budget terms, only the results pertaining to important terms are presented.

3.1. Circulation characteristics

Figure 2 depicts the geographical distribution of the vector wind at 850 and 200 hPa during the break and its departures from pre- and post-break phases of the summer monsoon, along with their t-test significance at the 95% confidence level (shaded region). Figure 2 (b) and (c) shows that, at the 850 hPa level in the monsoon trough zone, significantly stronger easterlies prevail during pre- and post-break periods and the easterlies extend well to the south of 30 °N. The easterlies in the post-break period are comparatively stronger and more extensive than in the pre-break period, particularly towards the eastern end. This may be due to the shifting of the monsoon trough to the foothills of the Himalayas. The cross-equatorial flow and the LLJ reaching the west coast of India from the Somali coast weakens during the break (Figure 2(a)). The significant low-level westerlies in the southern Bay of Bengal are found to be stronger in the post-break period than in the pre-break at 850 hPa. The weakening in the cross-equatorial flow and LLJ during the break period could be due to shifting and weakening of the seasonal low northwards, as indicated by the absence of low-level easterlies in the monsoon trough zone and by the weakening or displacement of the Mascarane high-pressure

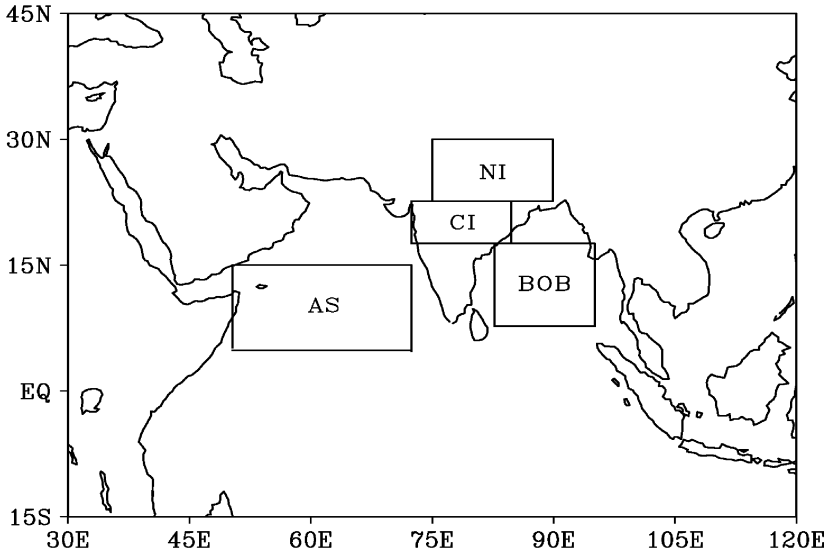

Figure 1. Geographical boundaries of the region of study with the four sectors shown, i.e. Arabian Sea (AS), Bay of Bengal (BOB), northern India (NI) and central India (CI)

cell in the southern Indian Ocean. The weakening of cross-equatorial flow and the LLJ during the break could also lead to less air–sea exchange and a reduction of water vapour in the atmosphere. The flow pattern at 200 hPa (Figure 2(d)–(f) indicates stronger easterlies during the pre- and post-break periods in the region 15 °S–10 °N, 45–75 °E. Though the differences in the region are not significant, they could possibly be due to a stronger return current in the upper levels in response to stronger cross-equatorial flow in the lower levels, as indicated by the 850 hPa flow. However, significant changes from the pre-break to the break situation are observed over Maharashtra and the adjoining Arabian Sea (Figure 2(e)). On the other hand, during the revival of the monsoon from the break to the post-break, significant departures are observed in a zonal belt of 10–15° extending from the eastern Bay of Bengal to the central Arabian Sea across the peninsula (Figure 2(f)).

Figure 3 shows the sectorial cross-sections of the zonal and meridional winds averaged over the latitudinal belts extending from 30 to 120 °E for the break and their departure from pre- and post-break periods along with their *t*-test significance. Figure 3(a) shows that low-level westerlies at 10 °N (900 hPa) are weaker during the break (i.e. LLJ weakens), whereas upper-level easterlies at 100 hPa close to 12–15 °N are stronger during the break. Figure 3(b) indicates a significant pre-break to break departure of zonal winds in two columns. The first column, located between 20 and 25 °N, surface to 200 hPa, indicates a significant negative departure of 0.5 to 1.5 m s^{-1}. The second column, located between 8 and 16 °N, surface to 300 hPa, shows a significant positive departure of about 1 m s^{-1}. Figure 3(c) shows a significant post-break to break departure of zonal wind. Here also, departures are noticed in the two columns. The first is located between 17 and 31 °N, surface to 400 hPa, and shows a negative departure of 0.5 to 1.5 m s^{-1}. The second column extends from 5 to 10 °N, surface to 100 hPa, and shows a positive departure of 0.5 to 1.5 m s^{-1}. These columnar departures are due to changes in the lower-level monsoonal westerlies and upper tropospheric easterlies. During the pre-break to break departure, westerlies from northern latitudes move southwards, whereas in the post-break to break, westerlies from southern latitudes move northwards, particularly between the surface and mid levels. Figure 3(d)–(f) shows the meridional wind during break and departures from pre-break to break and post-break to break. Significant but small departures are noted in Figure 3(e) in the meridional wind in the 700 to 400 hPa layer, between 15 °S and 10 °N.

The geographical distribution of the omega field at 850 and 200 hPa during the break and its departure from pre- and post-break periods and tested for significance at the 95% confidence level are shown in Figure 4. During the break period (Figure 4(a)) there is a sinking motion at 850 hPa over the entire

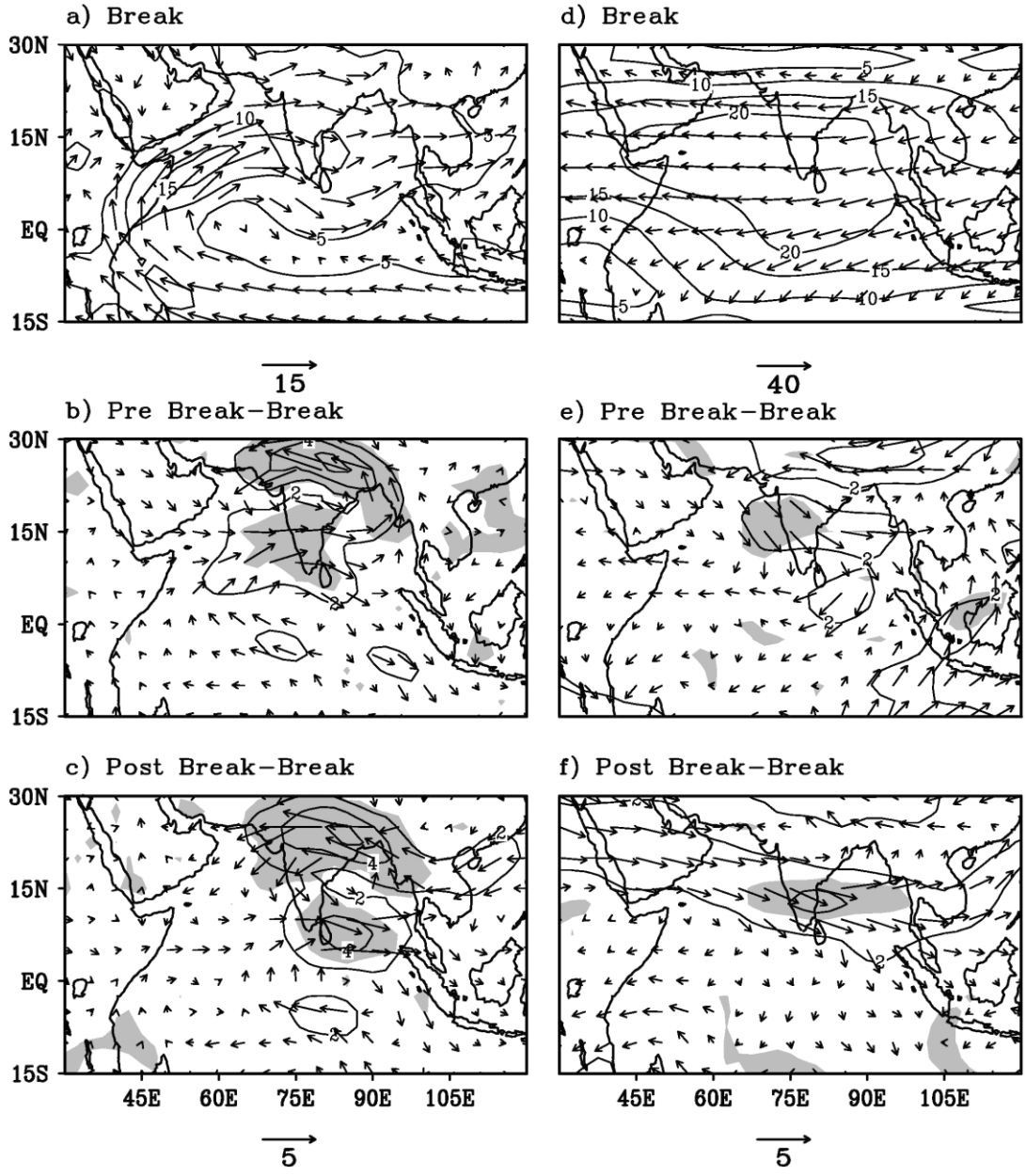

Figure 2. Geographical distributions of vector wind field (m s^{-1}) at 850 hPa for (a) break, (b) pre-break–break, (c) post-break–break. (d), (e) and (f) Same as (a), (b) and (c) respectively, but for 200 hPa with confidence limits above 95% (shaded)

country, except for a smaller area in the Arabian Sea off the Maharashtra coast and the eastern Bay of Bengal off the Mayanmar coast, where a rising motion is noticed. Departures from pre- and post-break periods (Figure 4(b) and (c)) indicate a significant strong upward motion of $(20–30) \times 10^{-3}$ Pa s^{-1} in the entire monsoon trough zone, as well as over most parts of the country. This could be due to the location of the monsoon trough south of the foothills of the Himalayas during the pre- and post-break periods, resulting in convergence and hence a higher vertical upward velocity. At 200 hPa (Figure 4(d)), the major portion of the country continues to be a region of sinking motion during the break phase, except for the Bay of Bengal and the northern Indian Ocean. During pre- and post-break departures (Fig. 4(e)

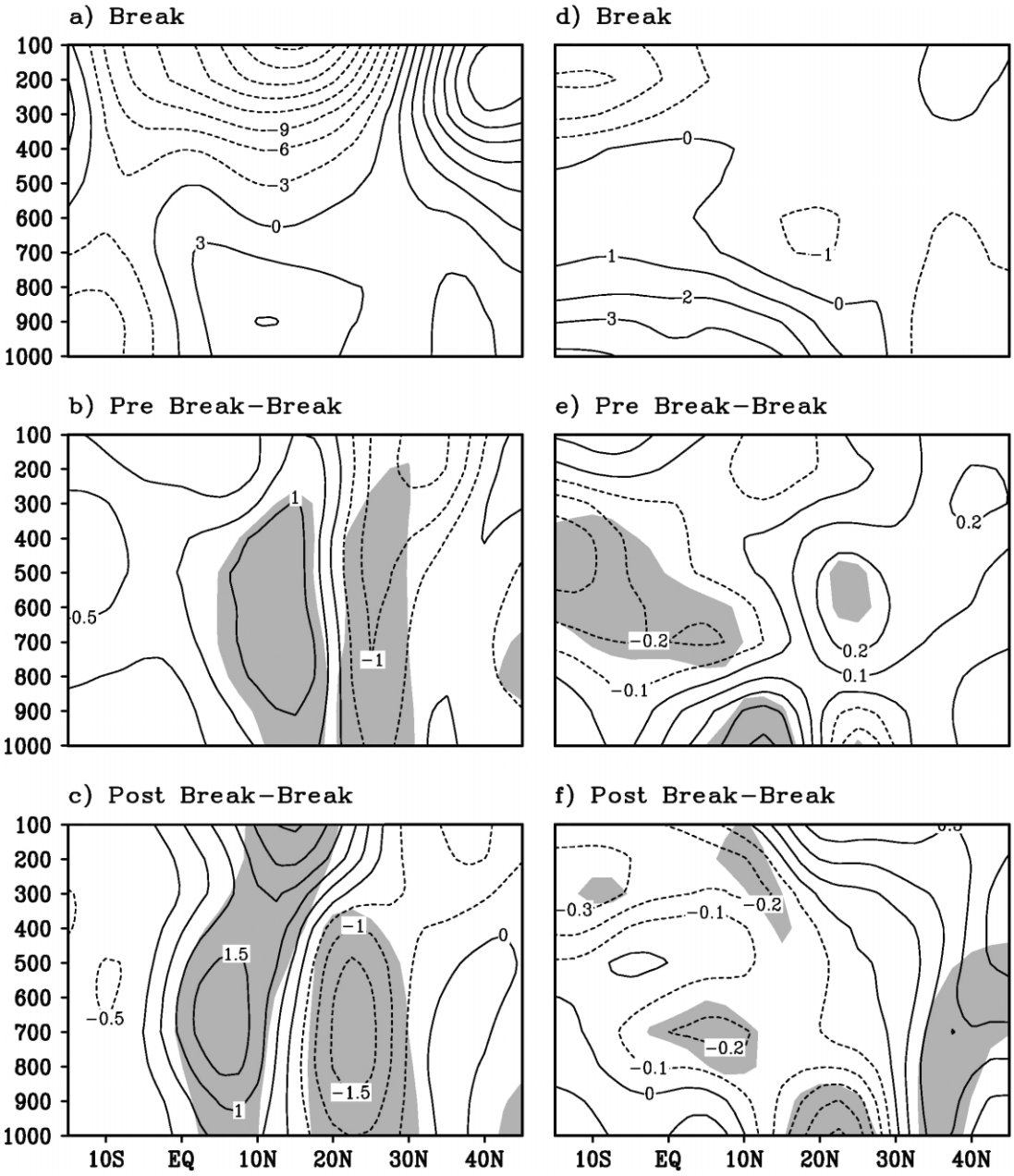

Figure 3. Sectorial mean (30–120 °E) vertical cross-sections of zonal wind (m s^{-1}) for (a) break (b) pre-break–break, (c) post-break–break. (d), (e) and (f) Same as (a), (b) and (c) respectively, but for meridional wind (m s^{-1}) with confidence limits above 95% (shaded)

and (f)), significant upward motion is indicated in the monsoon trough zone, and more so in the Bay of Bengal. Thus, at 200 hPa, upward motion continues to be shown in the Bay of Bengal in pre-break, break and post-break periods, though the magnitudes in the pre- and post-break are higher. This possibly explains why the Bay of Bengal remains convectively active even during break-monsoon situations. Further, this could also be due to the entrance region of the tropical easterly jet being located over the eastern Bay of Bengal, leading to persistent divergence, as indicated by Figure 2(d)–(f) during pre- to post-break periods.

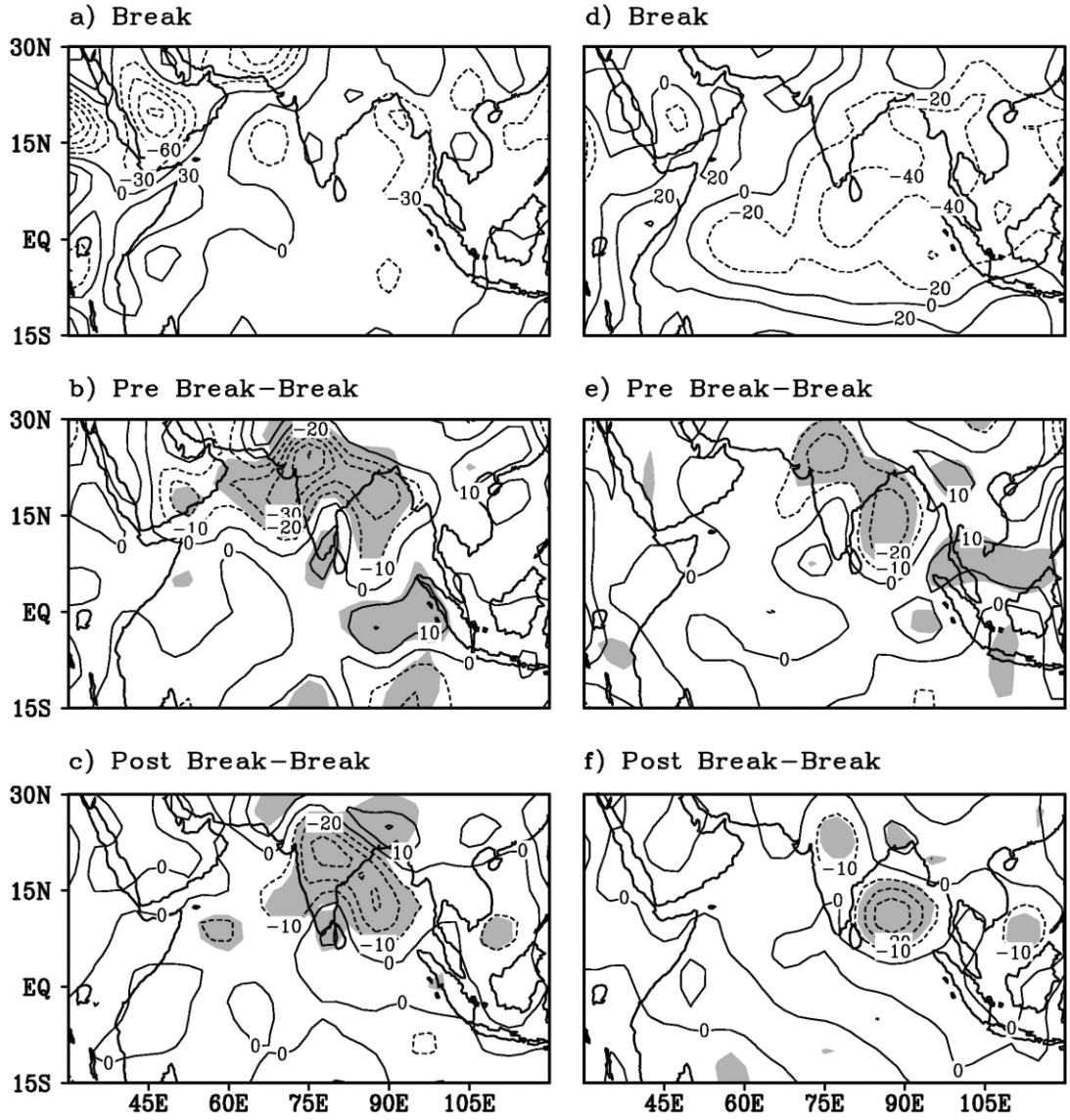

Figure 4. Geographical distributions of vertical velocity (10^{-3} Pa s^{-1}) at 850 hPa for (a) break, (b) pre-break–break, (c) post-break–break. (d), (e) and (f) Same as (a), (b) and (c) respectively, but for 200 hPa with confidence limits above 95% (shaded)

The sectorial mean cross-section of the omega field is depicted in Figure 5, which shows that omega weakens during the break monsoon between 15 and 20 °N, indicating a weakening of the Hadley cell. Figure 5(b) indicates that, with the approach of a break, rising upward motion increases significantly in the 5–10 °N belt and sinking motion increases in the 10–25 °N belt. Proceeding from break to post-break, the upward motion increases in the 10–25 °N belt (Figure 5(c)).

The distributions of vorticity at 850 and 200 hPa during the break phase and their departures during pre- and post-break phases, and with their *t*-test results, are shown in Figure 6. It is clear from Figure 6(a)–(c) that the anticyclonic vorticity at 850 hPa in the southern and southeastern Arabian Sea is less during a break than during pre- or post-break periods. This may be due to the weakening of the anticyclonic circulation associated with the southern Indian Ocean anticyclone. Significantly strong cyclonic vorticity is observed in the monsoon trough zone extending from northwest India to the head of the Bay of Bengal during both pre- and post-break

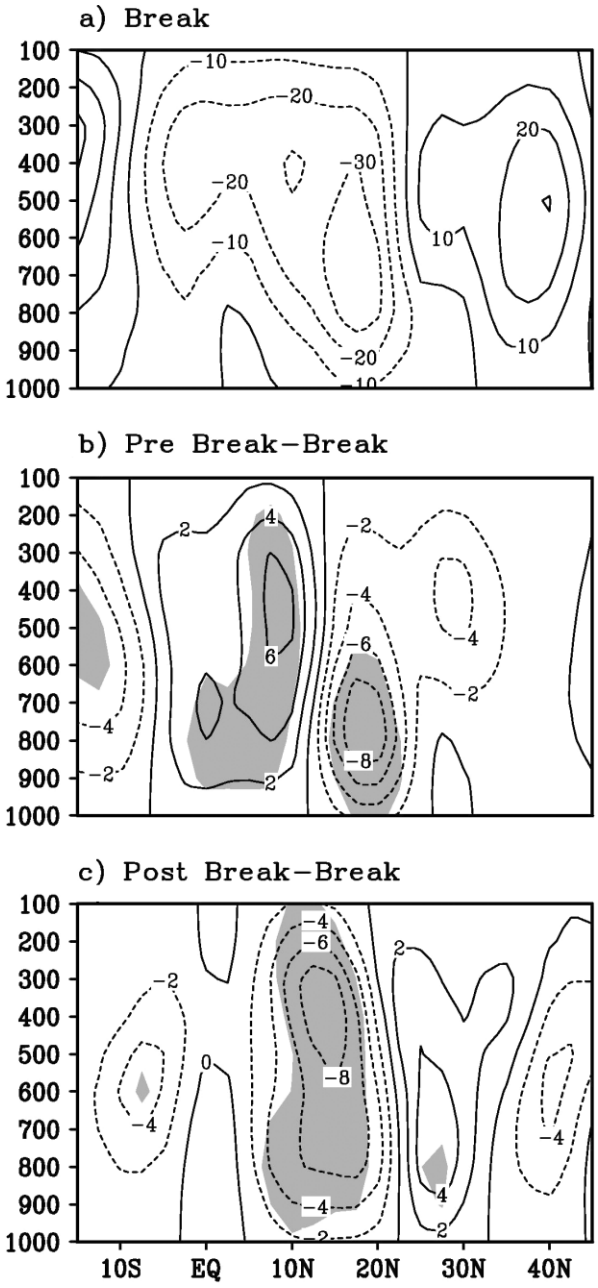

Figure 5. Sectorial mean (30–120 °E) vertical cross-sections of vertical velocity (10^{-3} Pa s^{-1}) for (a) break, (b) pre-break–break, (c) post-break–break with confidence limits above 95% (shaded)

departures (Figure 6(b) and (c)). It is also supported by the omega field at 850 hPa shown in Figure 4(a)–(c). In the equatorial region, particularly in the southwestern Arabian Sea, the reduction in the anticyclonic vorticity is due to weaker cross-equatorial flow during the break period. At 200 hPa (Figure 6(d)–(f)), significant but comparatively weaker anticyclonic vorticity prevails over the monsoon trough during the pre- and post-break periods. This could be due to the weakening of easterlies associated with the weakening of Tibetan anticyclones, as is indicated by the departures.

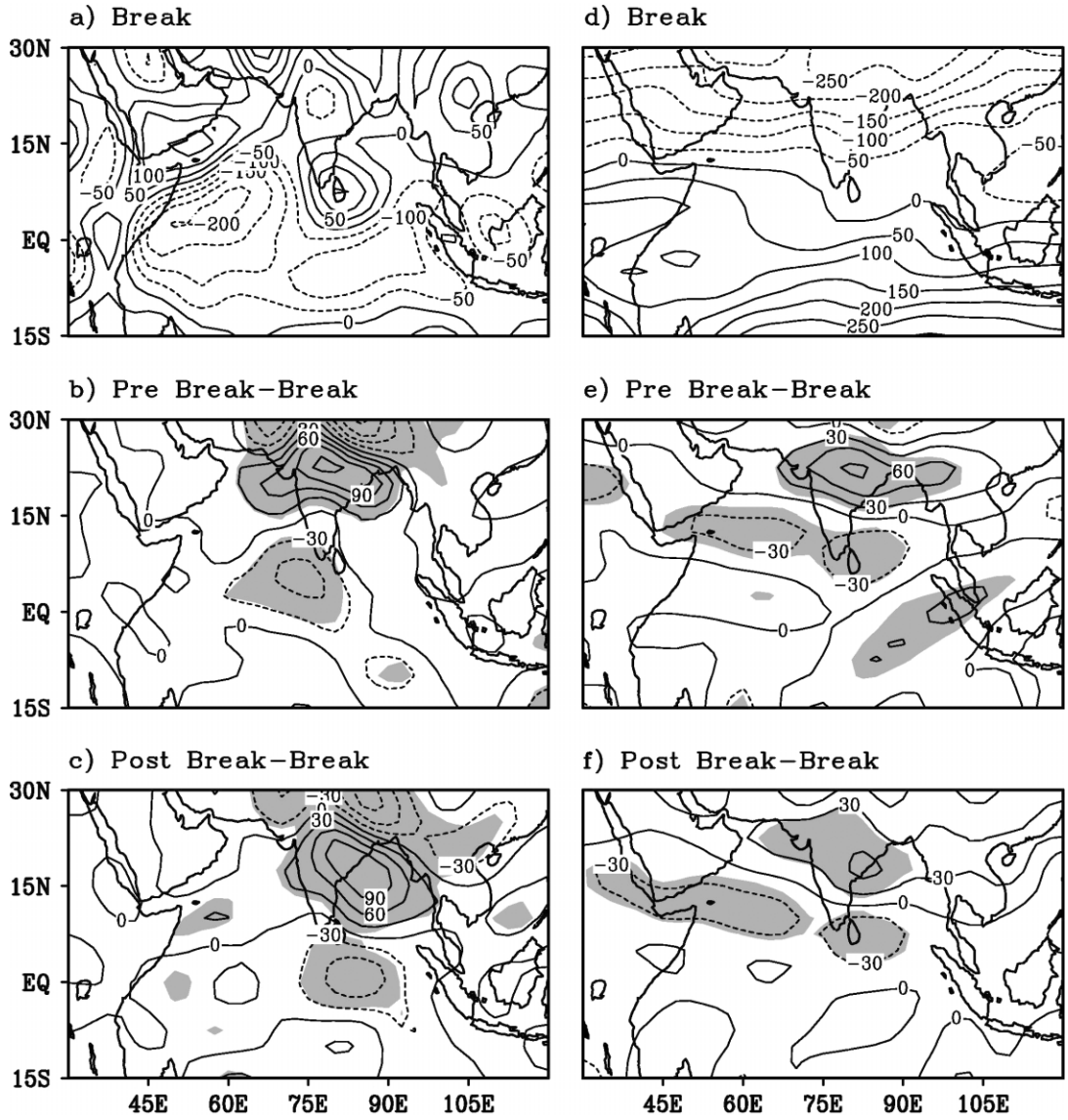

Figure 6. Geographical distributions of vorticity (10^{-7} s^{-1}) at 850 hPa for (a) break, (b) pre-break−break, (c) post-break−break. (d), (e) and (f) Same as (a), (b) and (c) respectively, but for 200 hPa) with confidence limits above 95% (shaded)

3.2. KE budget

The distribution of vertically integrated (1000−100 hPa) horizontal flux divergence of KE during the break period and its departure during pre- and post-break periods, along with the *t*-test results, are shown in Figure 7(a)−(c). During the break period, the central and northeastern Bay of Bengal is the region of flux divergence of KE, but during the pre- and post-break departures the significant flux divergence region is in the southwestern Bay of Bengal and flux convergence occurs in the northeastern Bay of Bengal, as indicated by Figure 7(b) and (c). The northern and central Arabian Sea is the region of flux convergence of KE during the break period, and this weakens considerably during the pre- and post-break periods. The stronger flux convergence of KE in the Arabian Sea and flux divergence in the Bay of Bengal during the break period is due to the combined effect of the LLJ and the tropical upper tropospheric easterly jet, caused as a result of changes in the location of entrance/exit regions during different phases of the monsoon.

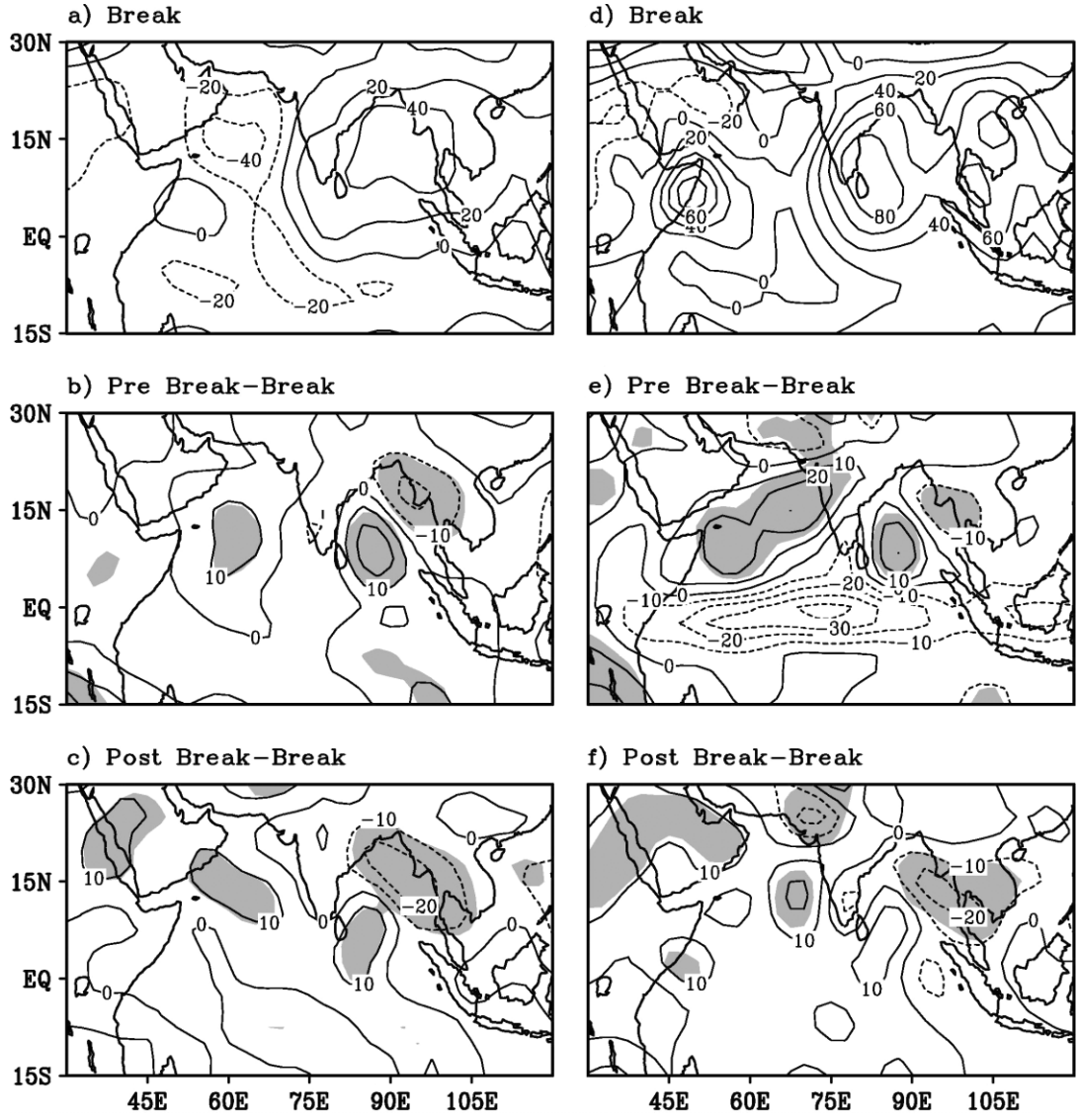

Figure 7. Geographical distributions of vertically integrated horizontal flux divergence of kinetic energy (10^{-1} W m^{-2}) for (a) break, (b) pre-break−break, (c) post-break−break. (d), (e) and (f) Same as (a), (b) and (c) respectively, but for adiabatic generation of kinetic energy (10^{-1} W m^{-2}) with confidence limits above 95% (shaded)

Figure 7(d)−(f) shows the distribution of vertically integrated adiabatic generation of KE during the break period and its departure during pre- and post-break periods, together with the *t*-test significance. Positive magnitudes denote the generation of KE through the conversion of APE, and negative magnitudes denote the destruction of KE, i.e. transformation of KE back to APE. The maximum noticed off East Africa is due to the presence of strong ageostrophic flow in that region. The generation maximum observed in the southwestern Bay of Bengal, off the Tamil Nadu and Sri Lanka, is also due to ageostrophic motion. The pre-break to break departures (Figure 7(e)) indicate that a significantly higher magnitude of generation takes place off the Konkan−Goa coasts and the southwestern Bay of Bengal, off Tamil Nadu and Sri Lankan coasts. In the post-break to break departure, significant generation of KE takes place over the northeastern Bay of Bengal and adjoining Mayanmar, northwestern India and less generation over the southeastern Arabian Sea and the Arabian Peninsula (Figure 7(f)). This is borne out through sea-level pressure and contour chart

analysis, particularly in the lower levels, where strong pressure gradients in the regions are observed with cross-isobaric flow. However, during the pre-break, in the equatorial zone, negative generation or very little positive generation is observed. In other words, this is a weak zone of generation of KE. In fact, the equator or the region south of it in the Indian Ocean is a region of weak generation of KE.

In order to understand the characteristic features of KE generation over the area of study, the two components of adiabatic generation of KE, namely the zonal adiabatic generation of KE and the meridional adiabatic generation of KE, are presented in Figure 8. Studies by Kung (1966a,b) indicated that the zonal component contributes to destruction of KE in the tropics and generation of KE in the extratropics. On the other hand, the meridional component contributes towards generation in the tropics and destruction in the extratropics. The zonal generation during the break (Figure 8(a)) indicates destruction over and off Arabia and the northeastern Bay of Bengal and its neighbourhood, but strong generation is indicated over the Indian land mass, particularly the southern peninsula. However, in the monsoon domain, the zonal component leads to generation and destruction of KE. Moreover, significantly higher destruction is observed over the northeastern Bay of Bengal during pre- and post-break departures (Figure 8(b) and (c)).

Figure 8(d)–(f) indicates generation of KE due to meridional motion during the break monsoon and its departures from pre- and post-break periods. During the break phase, the meridional component leads to the generation of KE over and off the East African coast and the northeastern Bay of Bengal and adjoining Mayanmar. Significantly higher generation of KE due to the meridional component is observed in the Arabian Sea over and off the Somali coast and the Bay of Bengal during the pre-break phase (Figure 8(e)). Negative generation is also observed in the equatorial zone between 45 and 120 °E. This negative generation is absent during the post-break periods. Significant negative generation is observed over Bangladesh and the adjoining region and the southern Bay of Bengal during pre- and post-break departures (Figure 8(e) and (f)).

3.3. Vorticity budget

Figure 9 shows the distribution of vertically integrated horizontal advection of planetary and relative vorticity during the break and its departures during pre- and post-break periods tested for their significance at the 95% confidence level. Figure 9(a)–(c) indicates that significantly larger cyclonic vorticity due to planetary motion is advected over the head of the Bay of Bengal region, and the monsoon trough zone during the pre- and post-break periods could be due to advection of air coming from higher latitudes, and this probably happens in the upper troposphere. The advection of relative vorticity is significant during pre- and post-break departures over the Indian land mass and the Bay of Bengal (Figure 9(e) and (f)). The advection is cyclonic in the Arabian Sea and there is anticyclonic vorticity in the Bay of Bengal. The probable reason appears to be the strong low-level westerlies associated with the LLJ that are associated with marked changes in the sign of curvature when crossing over to the Bay of Bengal from the Arabian Sea across the southern peninsula.

3.4. Heat and moisture budget

The geographical distribution of vertically integrated horizontal flux of heat between 1000 and 100 hPa during the break and its departures during pre- and post-break periods are shown in Figure 10(a)–(c). Horizontal flux convergence of heat of 400 to 600 W m^{-2} is observed over the Bay of Bengal and it extends into the South China Sea–western Pacific Ocean during the break period. During pre- and post-break departures (Figure 10(b) and (c)), significantly higher flux convergence of heat is observed in the monsoon trough compared with the break phase (Figure 10(a)). This possibly could be due to higher convergence of the moist air over the head of the Bay of Bengal and monsoon trough zone, leading to cloud formation and release of latent heat. The Pacific Ocean region shows less flux of heat. It appears as if, during the break phase, the region of heat flux convergence shifts eastwards from the Indian land mass.

The vertically integrated diabatic heating between 1000 and 100 hPa during the break and the departures from it during the pre- and post-break periods are shown in Figure 10(d)–(f). During the break phase, the northeastern Bay of Bengal and further northeastwards, extending into the South China Sea–Pacific Ocean, show diabatic heating of 200–300 W m^{-2}. During pre-break or post-break departures (Figure 10(e) and (f)),

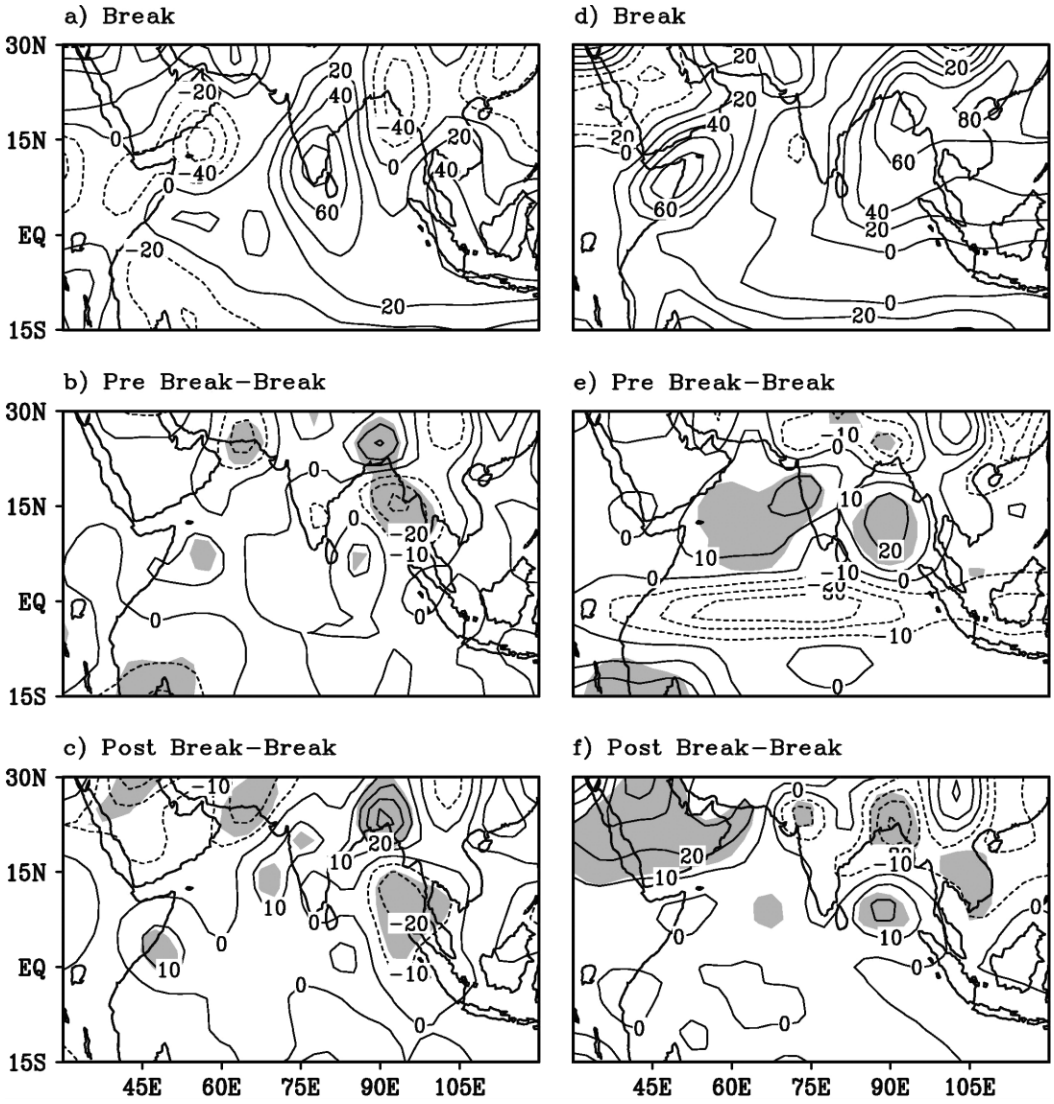

Figure 8. Geographical distributions of vertically integrated zonal adiabatic generation of kinetic energy (10^{-1} W m^{-2}) for (a) break, (b) pre-break–break, (c) post-break–break. (d), (e) and (f) Same as (a), (b) and (c) respectively, but for meridional adiabatic generation of kinetic energy (10^{-1} W m^{-2}) with confidence limits above 95% (shaded)

significantly higher diabatic heating is observed in the monsoon trough zone. The diabatic heating over the South China Sea–Pacific Ocean decreases. The diabatic heating is related to cloud formation and precipitation. During the pre- and post-break periods, a greater amount of cloud formation and associated precipitation in the monsoon trough zone would lead to higher diabatic heating.

The vertically integrated horizontal moisture flux during the break and departures from it during the pre- and post-break periods are shown in Figure 11(a)–(c). During the break phase, the northeastern Bay of Bengal and the region extending into the South China Sea–Pacific Ocean shows horizontal convergence of moisture flux of 100–200 W m^{-2}. During pre-break or post-break departures, significantly higher horizontal convergence of moisture flux is noticed in the monsoon trough zone over the Indian land mass (Figure 11(b) and (c)). Convergence of horizontal flux of moisture decreases over the Pacific Ocean–South China Sea during the pre- and post-break periods.

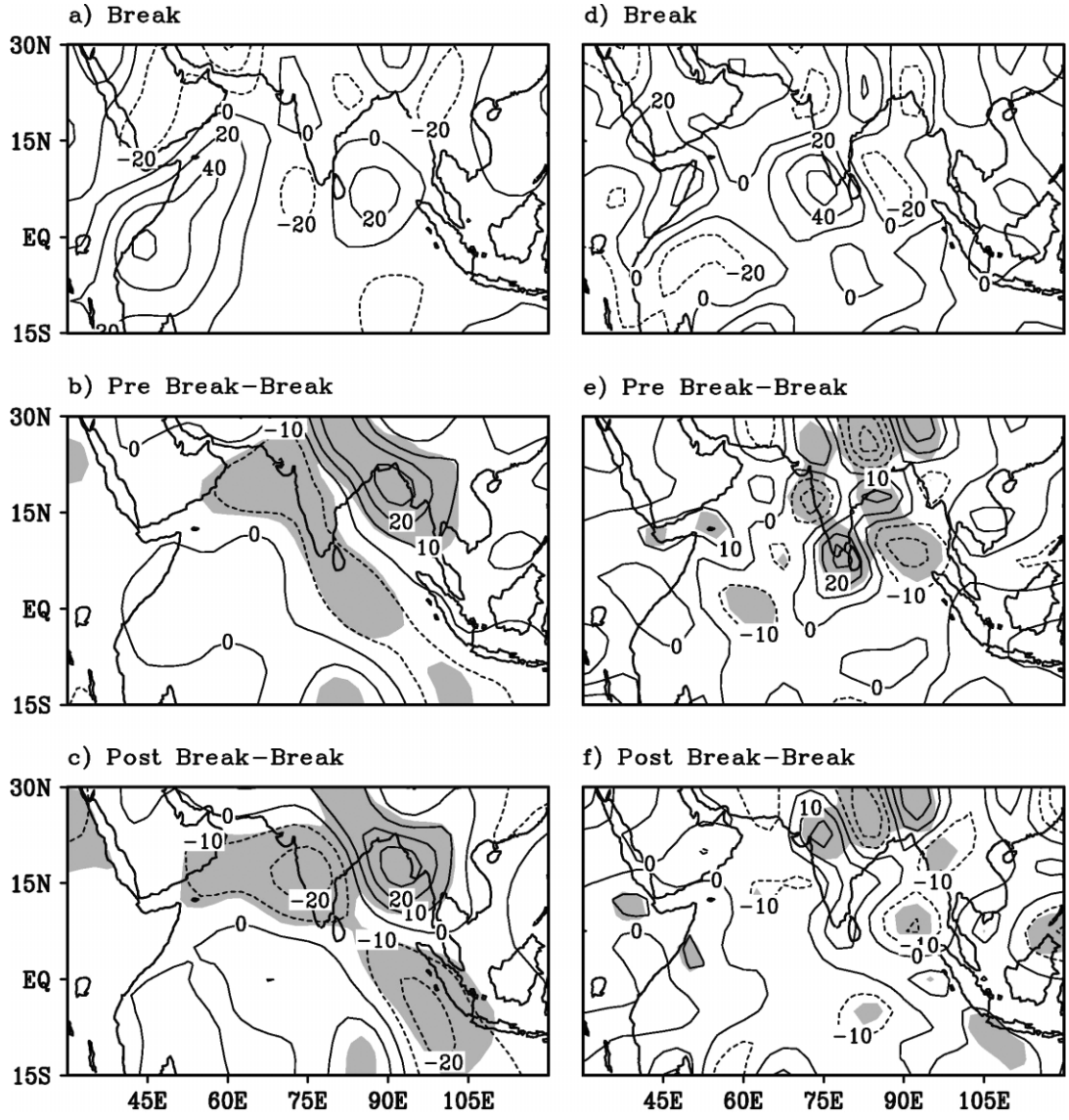

Figure 9. Geographical distributions of vertically integrated planetary vorticity advection (10^{-8} W m^{-2}) for (a) break, (b) pre-break–break, (c) post-break–break. (d), (e) and (f) Same as (a), (b) and (c) respectively, but for relative vorticity advection (10^{-8} W m^{-2}) with confidence limits above 95% (shaded)

3.5. Sectorial studies of some aspects of energetics

In Section 3.2, the energetic aspects of break-monsoon conditions were examined over the entire domain of the study at the grid points of analysis. In order to see the collective response for a specific region, integrated volume averages in respect of some of the budget terms are examined over four important sectors: Arabian Sea (AS), Bay of Bengal (BOB), central India (CI) and northern India (NI); see Figure 1.

Averages of horizontal flux of KE for the pre-break, break and post-break over the four significant sectors are shown in Figure 12(a). The horizontal flux of KE in the AS sector is convergent. However, during the break phase the convergence flux is higher than during the pre- and post-break epochs. The horizontal flux of KE is highly divergent in the BOB sector. The magnitude is of the order of 4.2 W m^{-2}. However, the flux gradually decreases from pre-break to post-break in the BOB sector. The horizontal flux of KE over the CI

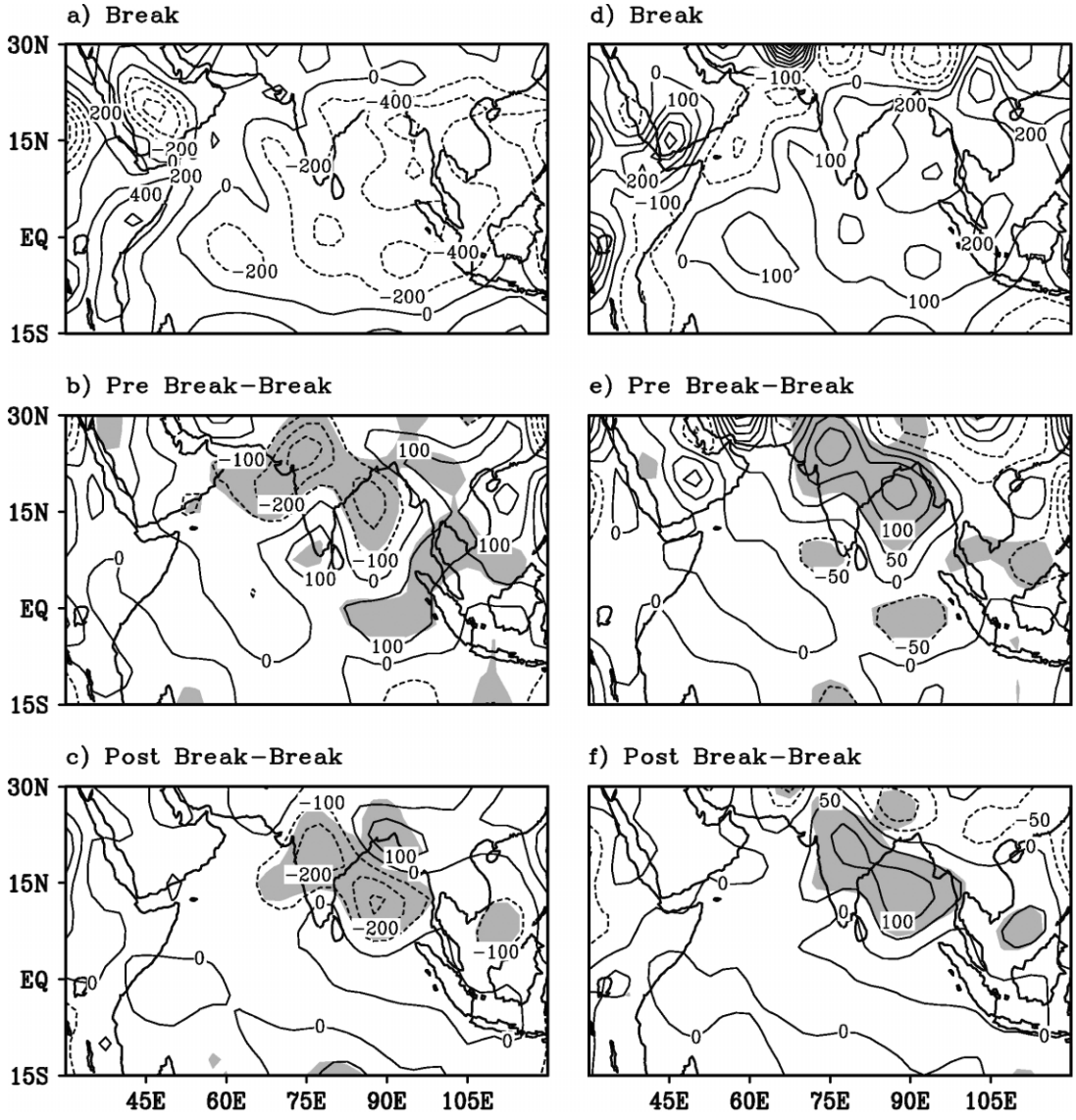

Figure 10. Geographical distributions of vertically integrated horizontal flux of heat (W m^{-2}) for (a) break, (b) pre-break–break, (c) post-break–break. (d), (e) and (f) Same as (a), (b) and (c) respectively, but for diabatic heating (W m^{-2}) with confidence limits above 95% (shaded)

sector is considerably less divergent than in the BOB sector and decreases from the pre- break to the break phase, but does not show any change subsequently. The horizontal flux of KE is weakly convergent and is at a minimum during the break period for the NI sector.

Figure 12(b) shows the average of the adiabatic generation of KE over the four sectors during the pre-break, break and break periods. The magnitude of the average of the generation of KE over the AS sector during the pre-break is 3 W m^{-2}; during the break this reduces to 1.5 W m^{-2}, and after the cessation of the break it increases to 2.3 W m^{-2}. Since the generation is due to cross-isobaric flow, it is evident that during the break the pressure gradient becomes slack in the AS sector. The generation of KE over the BOB sector during all three periods, i.e. before, during and after the break, is very high compared with the AS sector and shows a gradual continuous decrease. The magnitude varies between 7.0 and 6.0 W m^{-2}. The high magnitude and

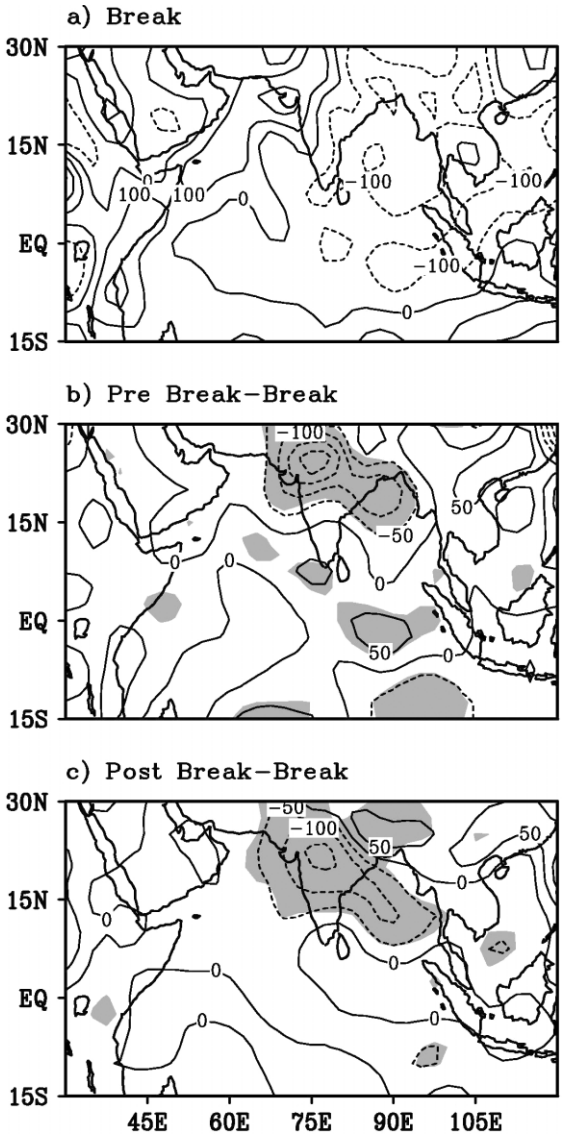

Figure 11. Geographical distributions of vertically integrated horizontal flux of moisture (W m^{-2}) for (a) break, (b) pre-break−break, (c) post-break−break with confidence limits above 95% (shaded)

slow continuous reduction indicates that a steeper pressure gradient and cross-isobaric flow continue to prevail in the BOB sector. The generation of KE in the CI sector shows patterns similar to the AS sector, except that the magnitude of generation is higher in the three phases. However, the generation is less than in the BOB sector. The magnitudes vary between 5.0 and 4.0 W m^{-2}. The generation of KE for all the sectors is lowest over the NI sector. The magnitude varies between 1.7 and 1.0 W m^{-2}. In other words, little variation in pressure gradient and cross-isobaric flow is observed over the NI sector.

Averages of adiabatic conversion of APE to KE for pre-break, break and post-break over the four sectors are shown in Figure 12(c). The adiabatic conversion of APE to KE is highest in the BOB sector, followed by the CI sector, and is least in the AS sector. The magnitude in the BOB and CI sectors ranges between 600 and 800 W m^{-2}. Over the NI sector, the conversion of APE to KE is negative, i.e. KE is being consumed. It is noticed that conversion from APE to KE is lower during the break period than in the pre- and post-break

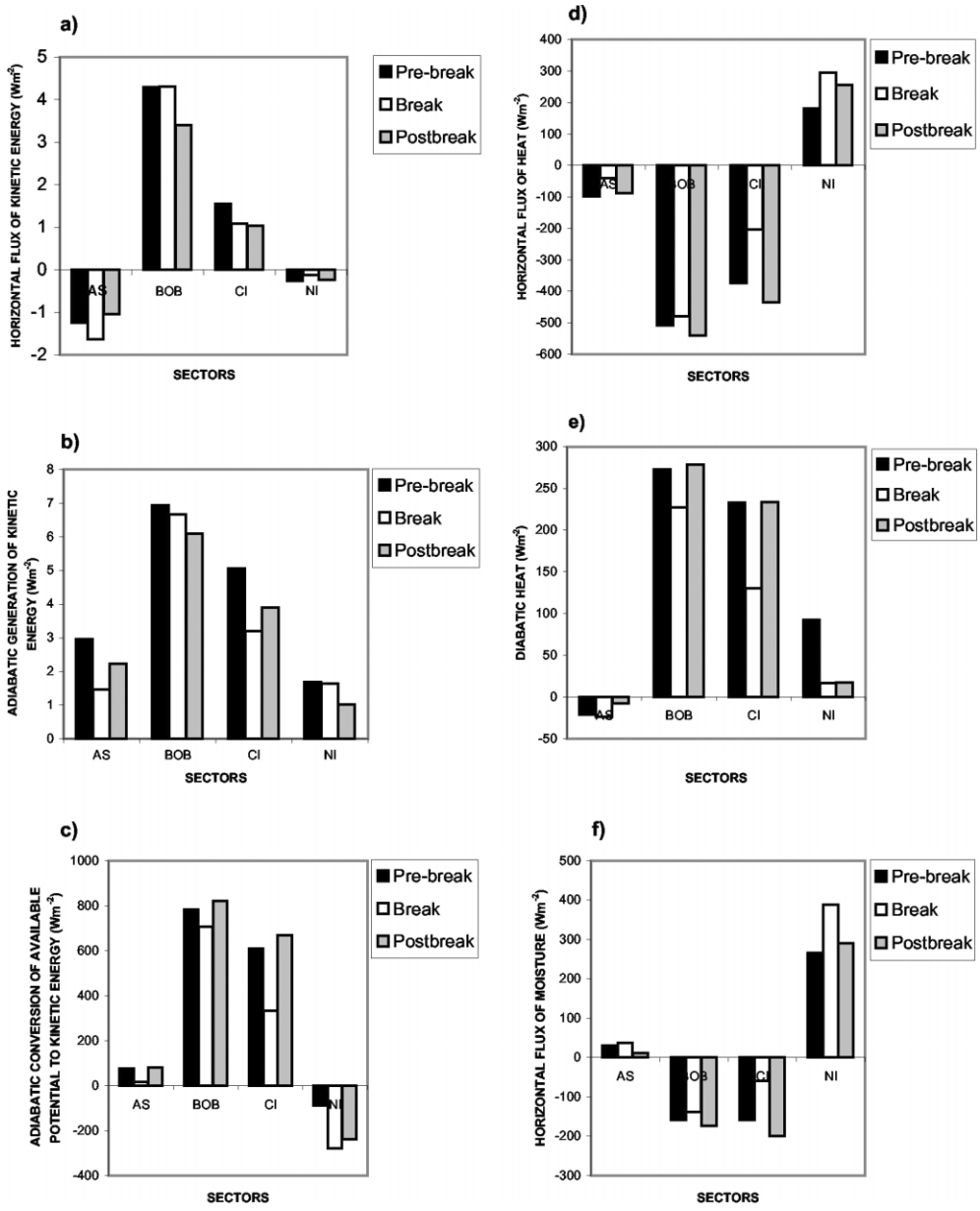

Figure 12. Variations (W m^{-2}) of vertically integrated (a) adiabatic generation of KE, (b) horizontal flux of KE, (c) horizontal flux of heat, (d) adiabatic conversion of APE to KE, (e) diabatic heating, (f) horizontal flux of moisture over the sectors AS, BOB, CI and NI for pre-break, break and post-break periods

periods. The probable reason appears to be that, convectively, the BOB and CI sectors are the most active regions. During the break, the convective activity decreases, causing a reduction in APE. The AS sector is not convectively active, except close to the west coast of India. The opposite behaviour of the NI sector, compared with the other sector, is due to the fact that this sector consists generally of an area north of the monsoon trough line, where sinking motion prevails.

Figure 12(d) shows the average of the horizontal flux of heat over the four sectors during the pre-break, break and post-break periods. The horizontal flux of heat is weakly convergent in the AS sector during the break period, as well as during pre- and post-break periods. Its magnitude is 50 W m^{-2} during the

break period. It is strongly convergent in the BOB sector in the pre- and post-break periods. Its magnitude (475 W m^{-2}) is less during the break period. The pattern followed in the CI sector is similar to that in the BOB sector and is less during the break phase. The horizontal heat flux pattern in NI sector is opposite to that of the AS, BOB and CI sectors, i.e. it is divergent in the pre-break, break and post-break periods. It is more during the break period, at 300 W m^{-2}.

Figure 12(e) shows the average of diabatic heat over the four sectors during the pre-break, break and post-break periods. The diabatic heating in the BOB and CI sectors is highest and varies between 200 and 300 W m^{-2}. It is a minimum over the NI sector and negative in the AS sector. As stated earlier, the convection is responsible for intense diabatic heating in the BOB and CI sectors. Over the NI sector, the convection is not large enough to cause intense heating. Over the AS sector, there is weak diabatic cooling, possibly due to evaporative cooling. The decrease in diabatic heating during the break period is due to a reduction in convection.

The averages of the horizontal flux of divergence of moisture for the pre-break, break and post-break periods over the four significant sectors are shown in Figure 12(f). The BOB and CI sectors are the regions of horizontal flux of convergence of moisture. The magnitude varies between 100 and 200 W m^{-2}. The NI sector is a very significant region of flux divergence of moisture, and the magnitude varies between 200 and 300 W m^{-2}. The AS sector is a very weak region of flux divergence of moisture. During the break period, the moisture flux convergence decreases over the BOB and CI sectors, whereas moisture flux divergence increases over the NI sector.

From examination of Figure 12, one may state that the BOB and CI sectors are the most active, where the magnitudes of generation of KE, horizontal flux of KE, horizontal flux of heat, conversion of APE to KE, diabatic heat and horizontal flux of divergence of moisture are highest. Further, the changes from pre-break to break and post-break are also most significant in these two regions. The changes in the CI sector are far sharper than in the BOB sector.

4. CONCLUSIONS

The results of this study clearly demonstrate a close consistency between dynamic and thermodynamic features during commencement/cessation of break situations along the monsoon trough. The broad conclusions are as follows.

Significant changes in the easterlies are observed at 850 hPa in the monsoon trough zone in the pre- and post-break departures. The easterlies to the north of the monsoon trough line during the post-break period are comparatively stronger and more extensive than in the pre-break period. Similarly, significant changes in the omega field and vorticity at 850 hPa are noticed in the monsoon trough zone, the coastal regions of western India and the southwestern Bay of Bengal, off the Tamil Nadu coast, during the pre-break to break and break to post-break periods.

At 200 hPa, significant upward motion and weaker anticyclonic vorticity are observed in the monsoon trough zone during the pre- and post-break periods, which is due to weakening of easterlies associated with the weakening of Tibetan anticyclones, as is indicated by the departures.

The zonal averaged wind field in the domain 30 to 120 °E indicates two belts, at 0–10 °N and 15–25 °N, where significant changes in zonal wind take place over the whole pre- to post-break period. Similar changes are also observed in the vertical velocity proceeding from the pre-break to break phase: the northern belt weakens and the southern belt strengthens. During the break to post-break period the process is reversed.

A stronger flux convergence of KE in the central Arabian Sea and flux divergence in the northeastern Bay of Bengal are observed during the break period, and this weakens considerably during the pre- and post-break periods. In order to understand the characteristic features of KE generation, the zonal component leads to a significantly higher destruction over the northeastern Bay of Bengal, whereas the meridional component leads to the generation of KE over the Bay of Bengal during the pre- and post-break departures.

Significant changes in the diabatic heating and in the horizontal flux of heat and moisture are observed in the monsoon trough zone, the central and northwestern Bay of Bengal from pre-break to break and its revival.

The reduction in the flux of moisture, horizontal flux of heat and diabatic heating are noticed in the monsoon trough zone from the pre-break to break periods. The moist easterlies to the north of the monsoon trough line are replaced by drier westerlies or northwesterlies in the monsoon trough zone in the lower and middle troposphere, and this leads to drying of the atmosphere and hence to a reduced flux of moisture, sensible heat and latent heat in the monsoon trough zone during the break period.

The energetics over the four different sectors examined indicate that the BOB and CI sectors are areas of higher magnitudes and changes from pre-break to break and break to post-break (in respect of generation of KE, horizontal flux of KE, horizontal flux of heat, conversion of APE to KE, diabatic heating and horizontal flux divergence of moisture) than the AS and NI sectors.

ACKNOWLEDGEMENTS

We wish to express our sincere thanks to NCEP–NCAR, USA, for providing the necessary data sets. We also gratefully acknowledge the Department of Science and Technology for financial support to complete the work.

REFERENCES

De US, Lele RR, Natu JC. 1998. Breaks in southwest monsoon. Pre-published Scientific Report No. 1998/3.

Kalnay E, Kanamitsu M, Kistler R, Collins W, Deaven D, Gandin L, Iredell M, Saha S, White G, Woollen J, Zhu Y, Chelliah M, Ebisuzaki W, Higgins W, Janowiak J, Mo KC, Ropelewski C, Wang J, Leetmaa A, Reynolds R, Jenne R, Joseph D. 1996. The NCEP/NCAR 40years reanalysis project. *Bulletin of the American Meteorological Society* **77**: 437–471.

Krishnamurti TN, Ardanuy P. 1980. The 10 to 20-day westward propagating mode and 'breaks in the monsoons'. *Tellus* **32**: 15–26.

Krishnan B, Zhang C, Sugi M. 2000. Dynamics of breaks in the Indian summer monsoon. *Journal of the Atmospheric Sciences* **37**: 1354–1372.

Koteswaram P. 1950. Upper levels lows in low latitudes in the Indian area during southwest monsoon season and breaks in monsoon. *Indian Journal of Meteorology and Geophysics* **1**: 162–164.

Kung EC. 1966a. Kinetic energy generation and dissipation in the large-scale atmospheric circulation. *Monthly Weather Review* **94**: 67–82.

Kung EC. 1966b. Large scale balance of kinetic energy in the atmosphere. *Monthly Weather Review* **94**: 627–640.

Malurkar SL. 1950. Notes on analysis of weather of India and neighborhood. Memoirs of Indian Meteorological Department, XXVLL, Part IV; 139–215.

Mukherjee AK, Natarajan G. 1968. Westward moving sea level low pressure systems in the south Bay of Bengal during southwest monsoon. *Indian Journal of Meteorology and Geophysics* **19**(3): 284–288.

Mohanty UC, Dube SK, Sinha PC. 1982a. On the large scale energetics in the onset and maintenance of summer monsoon — I: heat budget. *Mausam* **33**: 139–152.

Mohanty UC, Dube SK, Sinha PC. 1982b. On the large scale energetics in the onset and maintenance of summer monsoon — II: moisture budget. *Mausam* **33**: 285–294.

O'Brein JJ. 1970. Alternative solutions to classical vertical velocity problems. *Journal of Applied Meteorology* **9**: 197–203.

Pisharoty PR, Desai BN. 1956. Western disturbances and Indian weather. *Indian Journal of Meteorology and Geophysics* **7**: 333–338.

Ramamurthy K. 1969. Some aspects of 'break' in the Indian southwest monsoon during July and August. Forecasting manual. Indian Meteorological Department Publication, FMU, Rep. 4, 18.3.

Raman CRV, Rao YP. 1981. Blocking highs over Asia and monsoon droughts over India. *Nature* **289**: 221–223.

Ramaswamy C. 1962. Breaks in the India summer monsoon as a phenomenon of interaction between easterly and the subtropical westerly jet streams. *Tellus* **14**: 337–349.

Ramaswamy C, Pareek RS. 1978. The south-west monsoon over India and its teleconnections with the middle and upper tropospheric flow patterns over the Southern Hemisphere. *Tellus* **30**: 126–135.

Rao YP. 1976. *Southwest Monsoon*. Meteorology Monograph No. 1. India Meteorological Department: 1–367.

Rodwell MJ. 1997. Breaks in the Asian monsoon: the influence of Southern Hemisphere weather systems. *Journal of the Atmospheric Sciences* **54**: 2597–2611.

Unninayar MS, Murakami T. 1978. Temporal variations in the northern hemispheric summer monsoon circulations. *Indian Journal of Meteorology, Hydrology and Geophysics* **29**: 170–186.

